Proc. Natl. Acad. Sci. USA
Vol. 91, pp. 11148–11152, November 1994
Biochemistry

Pseudoknot in the central domain of small subunit ribosomal RNA is essential for translation

(protein synthesis/rRNA/RNA structure/ribosome)

ANTON VILA*, JUNESSE VIRIL-FARLEY, AND WILLIAM E. TAPPRICH†

Biology Department, University of Nebraska at Omaha, Omaha, NE 68182

Communicated by Carl R. Woese, June 17, 1994

ABSTRACT **Phylogenetic comparison of rRNA sequences has suggested that a pseudoknot structure exists in the central domain of small-subunit rRNA. In *Escherichia coli* 16S rRNA, this pseudoknot would form when positions 570 and 571 pair with positions 865 and 866. Mutations were introduced into this pseudoknot at the phylogenetically invariant nucleotides U571 and A865. Single mutations of U to A at 571 or A to U at 865 dramatically altered the structural stability of the 30S subunit and also impaired the function of the subunit in translation. When the mutations were combined to create a compensatory pairing, the normal structure of the 30S subunit was restored, and the function of the mutant subunit in translation returned to wild-type levels. These results demonstrate the existence of a higher order structure in rRNA that directly affects the folding of the 30S subunit. Given the position of this structure in the three-dimensional model of the small subunit and the additional interactions that are likely to form in the same rRNA region, the central domain pseudoknot appears to contribute to a complex structure of rRNA that controls the conformational state of the ribosome.**

Complete understanding of the mechanism of translation will require knowledge of the structure and function of the ribosome. In recent years, it has become apparent that rRNA is responsible for many of the structural features and functional activities of the ribosome (reviewed in ref. 1). To solve the structure of the ribosome, attention has focused on the folding of the rRNA within the ribosomal subunits (2–5). Constraints for this folding have been provided primarily by RNA–RNA crosslinking and chemical protection studies. Presently, it is possible to add specific tertiary interaction sites between rRNA residues to these folding constraints (6, 7).

Using a database of more than 1000 sequences, comparative analysis has revealed numerous potential tertiary interactions in rRNA (8–10). These interactions, if verified experimentally, will help to define the three-dimensional folding of rRNA domains within the ribosome. Such interactions are also likely to contribute to the dynamic conformational changes that may occur in the ribosome during protein synthesis. One type of tertiary interaction that has been identified by comparative sequence analysis is the pseudoknot, defined as a Watson–Crick pairing between nucleotides in a single-stranded loop and a complementary region outside of the loop (11). Pseudoknot motifs are common in rRNA, occurring 18 times in a recent structural model by Gutell *et al.* (12). For a few of these pseudoknots, a clear link between structure and function has been established. In the small subunit, pseudoknots are important for the initiation of protein synthesis and decoding at the ribosomal A site (6, 7).

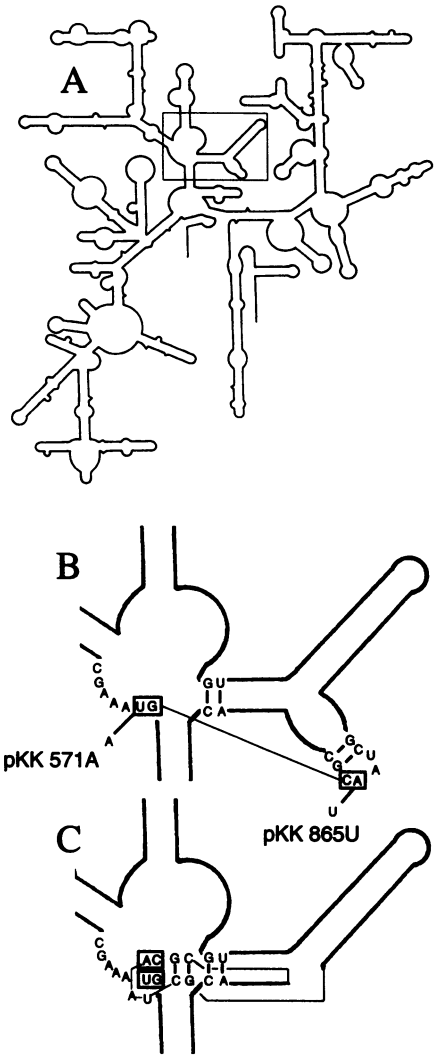

FIG. 1. Proposed structure for the central domain pseudoknot. (*A*) Secondary structure model for 16S rRNA. The region of the central domain which contains the pseudoknot is highlighted. (*B*) Detailed structure of the highlighted region showing the nucleotides surrounding positions 571 and 865. Nucleotides U571 and A865 are within the boxes that identify the pseudoknot participants. Also indicated are the single base substitutions constructed in this study. (*C*) Folding of the 571 and 865 regions into a coaxially stacked pseudoknot helix. This structure is modeled after Stern *et al.* (3).

In the large subunit, a pseudoknot is involved in ribosomal protein binding (13).

The publication costs of this article were defrayed in part by page charge payment. This article must therefore be hereby marked "*advertisement*" in accordance with 18 U.S.C. §1734 solely to indicate this fact.

*Present address: Department of Biochemistry, Brown University, Providence, RI 02912.
†To whom reprint requests should be addressed.

In the 16S rRNA of *Escherichia coli* ribosomes, three pseudoknots have been proposed by comparative sequence analysis (8, 9). Two of these structures have been confirmed experimentally by compensatory mutagenesis (6, 7). The present study investigates the third 16S rRNA pseudoknot. This structure involves base pairs between residues 570–571 and 865–866 in the central domain of 16S rRNA (Fig. 1). Numerous covariant base changes in rRNA sequences support the interaction between positions 570 and 866 (represented as 570·866; Table 1). The adjacent pair, involving positions 571 and 865 (571·865) is also proposed to be part of the pseudoknot interaction, even though no covariant changes have been reported for this pairing. Both U571 and A865 are phylogenetically invariant. Based on the strong phylogenetic evidence for the 570·866 pair, Stern *et al.* (3) have proposed a structure for the pseudoknot in three dimensions and included it in their model of the small ribosomal subunit. According to the model, the helix created by the pseudoknot, as well as the two-base stem underlying the 865 loop, stack coaxially on the secondary-structure helix closed by the base pair formed by residues 821 and 879 (821·879) (see Fig. 1). This extended structure occupies a position in the interior of the subunit near the base of the 30S subunit cleft (3).

To investigate the potential tertiary interaction between residues 570–571 and 865–866, site-directed mutations were constructed in the 571·865 pair. The effects of these mutations on the structure and function of the ribosome clearly demonstrate the existence and functional significance of the pseudoknot structure. Mutations that disrupt the 571·865 pair destabilize the folded structure of the 30S subunit and impair the ability of the mutant ribosomes to participate in translation. Compensatory mutations, which restore the pairing potential of 571 and 865, also restore structural stability and functional activity. The results suggest that the (570–571)·(865–866) pseudoknot contributes to a complex structure of rRNA that mediates the three-dimensional conformation of the 30S subunit.

MATERIALS AND METHODS

Construction of rRNA Mutations. Site-directed substitutions at positions 571 (U to A) and 865 (A to U) were constructed by oligonucleotide-directed mutagenesis (14). The mutations were confirmed by dideoxy sequencing (15). The A571 and U865 mutations were cloned into pKK3535 (16) to form the mutant expression plasmids pKK571A, pKK865U, and pKK571A·865U. A substitution at position 1192 of 16S rRNA (C to U), which confers spectinomycin resistance to plasmid-encoded ribosomes (17, 18), was cloned separately into each of the pKK3535 constructs to form pKK571A-1192U, pKK865U-1192U, and pKK571A·865U-1192U. All expression plasmids were transformed into *E. coli* strain DH1.

Preparation of Ribosomes and Ribosomal Subunits. Ribosomes were isolated from DH1 transformed with pKK3535 and the mutant derivatives. Cultures containing 500 ml of Luria-Bertani (LB) broth with 200 μg of ampicillin per ml were harvested in midlogarithmic growth phase (OD_{600} = 0.6). Tight-couple 70S ribosomes were prepared as described (19) and stored in small aliquots at −70°C in tight-couple 70S buffer (25 mM Tris·HCl, pH 7.6/6 mM $MgCl_2$/ 60 mM KCl). To isolate free 30S subunits, the tight-couple ribosomes were dialyzed overnight at 4°C against a buffer containing 25 mM Tris·HCl (pH 7.6), 1.5 mM $MgCl_2$, and 150 mM KCl. The dialyzed samples were fractionated in a 5–30% sucrose density gradient in the same buffer. Polyribosomes were prepared from cell lysates as described (20). Total cellular RNA was also isolated from the cell lysates by phenol extraction. Ribosomal RNA from pooled fractions of 30S subunits, 70S ribosomes, and polyribosomes was obtained by phenol extraction.

Growth Experiments. Bacterial growth was monitored by determining the turbidity of cultures using a Klett–Sommerson colorimeter. Cultures containing 50 ml of LB broth with 200 μg of ampicillin per ml were inoculated with bacteria resuspended from an agar plate to obtain an initial turbidity reading between 10 and 20. These cultures were incubated with shaking at the indicated temperature. Doubling times were calculated from plots of the logarithmic phase of the growth curves.

Quantitation of Mutant rRNA. The level of mutant rRNA in ribosomal pools was determined by using the primer extension method described by Sigmund *et al.* (21). The oligonucleotides used for primer extension analysis of positions 571 and 865 were 5′-CAAACCGCCTGCGTGCGCTTT-3′ and 5′-CCCAGGCGGTCGACTTAACGC-3′, respectively. The relative amounts of extension products were quantified with a Molecular Dynamics 425B PhosphorImager.

Table 1. Phylogenetic comparison of positions 570 and 866 in small-subunit rRNA (from ref. 29)

Source of ribosomes	Base pair 570·866, no. of examples			
	G·C	A·U	U·A	C·G
Eubacteria	394	2	53	0
Eucarya	0	0	251	0
Archaea	0	0	9	34
Mitochondria	32	0	3	1

Positions 571 and 865 are invariant in all species that have been sequenced.

RESULTS

Effects of rRNA Mutations on Cell Growth. The pseudoknot interaction involving the 571·865 pair was investigated by constructing compensatory mutations in a plasmid-coded copy of the rRNA operon. Single mutations of U to A at position 571 and A to U at position 865 were introduced to disrupt the potential pair (Fig. 1). These mutations were then combined to create a compensatory double mutant that restored the pairing potential with different nucleotides. Two different plasmids were used to express mutant rRNA within DH1. In plasmid pKK3535, rRNA from the *rrnB* operon is under the control of the native ribosomal promoters P_1P_2 (16). Cells containing this plasmid typically show a level of plasmid-encoded rRNA between 60% and 80% (22, 23). The second plasmid, pKK1192U, is a derivative of pKK3535 that contains a C-to-T transition at position 1192 of the 16S gene. While expression levels are the same as those of pKK3535, ribosomes containing U1192 are resistant to the antibiotic spectinomycin (17, 18). Thus, the addition of spectinomycin to cultures containing pKK1192U allowed ribosomes that contained the resistant, plasmid-encoded rRNA to be characterized *in vivo* without the interference of ribosomes that contained sensitive, chromosomally encoded rRNA.

Table 2. Growth rates of cells containing wild-type and mutant plasmids

Plasmid	Doubling time, min		
	at 30°C	at 37°C	at 42°C
pKK3535	56 ± 3	45 ± 2	33 ± 3
pKK571A	197 ± 16	94 ± 9	118 ± 13
pKK865U	132 ± 3	83 ± 5	49 ± 3
pKK571A-865U	92 ± 4	48 ± 11	40 ± 3

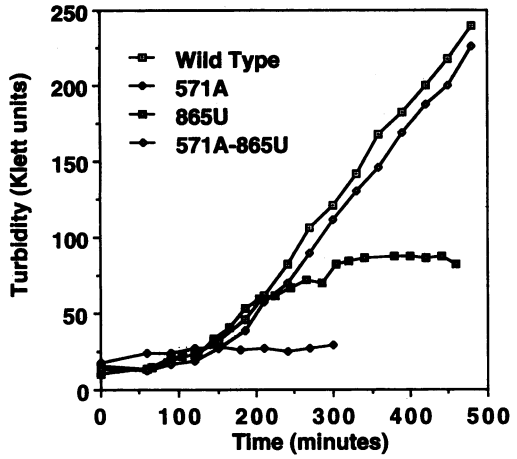

FIG. 2. Growth characteristics of cells containing wild-type and mutant plasmids in the presence of spectinomycin. The A571 and U865 mutations were cloned into a derivative of pKK3535, which contains the spectinomycin-resistance mutation of C to U at position 1192. The cultures of mutant and wild-type cells were grown at 37°C in LB broth with 200 μg of ampicillin and 100 μg of spectinomycin per ml.

The growth characteristics of cells containing the mutations in pKK3535 clearly demonstrated the importance of Watson–Crick complementarity between positions 571 and 865. When grown at 37°C, both single mutations (A571 and U865) severely impaired cell growth, while the double, compensatory mutation (A571·U865) restored the growth rate to the wild-type level (Table 2). This result was dramatically confirmed when cells were forced to use the mutant ribosomes exclusively. When grown in spectinomycin, pKK571A-1192U was lethal to the cell and pKK865U-1192U allowed approximately three doublings before cell death (Fig. 2). The compensatory double mutant, on the other hand, grew normally with a doubling time indistinguishable from cells containing pKK1192U. Thus, lethal mutations at either 571 or 865 were rescued to normal growth phenotype by a compensatory base change at the opposing position.

Growth rates for the pKK3535 constructs were also monitored at 42°C and 30°C (Table 2). In both cases, the A571 mutation was more deleterious than the U865 mutation. At the higher temperature, the deleterious growth phenotype of the A571 mutation was more pronounced when compared with growth at 37°C. The U865 mutation, on the other hand, was less deleterious to cell growth at 42°C than at 37°C. Still, at 42°C both single mutations displayed longer doubling times than did wild type, and the double mutation rescued the slow growth phenotype of each single mutation. At the lower temperature, both single mutations were extremely harmful to the cell. In this case, the double mutation was not as efficient in rescuing the slow growth phenotype but did improve growth significantly.

Effects of rRNA Mutations on Ribosome Structure. Ribosomes were isolated from cells containing the pKK3535 mutant constructs grown to midlogarithmic phase (A_{600} = 0.6) at 37°C. When the ribosomes were isolated under conditions that maintain 70S particles (6 mM $MgCl_2$), there were no differences in the sucrose gradient profiles among the wild-type and mutant preparations (data not shown). Primer extension analysis on the rRNA derived from these ribosomes showed that ≈60% of each ribosome preparation was plasmid-encoded mutant rRNA (Table 3). The level of mutant rRNA in these ribosomes correlated with the total amount of mutant rRNA expressed in the cells (Table 3). These results indicated that the mutant rRNA was efficiently assembled into association-competent 30S subunits. None of the mutations led to significant defects in rRNA expression or assembly.

To observe isolated 30S subunits, the ribosome preparations were dialyzed in a buffer containing 1.5 mM $MgCl_2$ and 150 mM KCl. Under these conditions 70S particles dissociate into subunits. After dialysis the subunits were separated by sucrose density gradient centrifugation. The low Mg^{2+} concentration led to a small population of unfolded 30S subunits in the wild-type sample (Fig. 3). The profiles of the subunits containing A571 and U865 both showed a significant increase in the concentration of unfolded subunits (Fig. 3). Primer extension analysis showed that the unfolded 30S particles contained primarily mutant 16S, whereas the folded 30S pool contained the majority of the wild-type 16S rRNA (Table 3). Thus, the single mutations produced a 30S subunit that was more susceptible to unfolding at the low Mg^{2+} concentration.

Under the same conditions of low Mg^{2+}, ribosomes containing the compensatory double mutation produced a sucrose gradient profile that was indistinguishable from wild type. Interestingly, the small pool of unfolded subunits in the double-mutant sample was somewhat enriched for plasmid-encoded rRNA (Table 3). However, since the vast majority of the subunits from the gradient were folded, on the whole, most of the double-mutant rRNA resided in the folded subunits.

The unfolded 30S subunits for both single mutations were tested in subunit association assays. Neither mutation inhibited subunit association, when the Mg^{2+} concentration was raised to 6 mM (data not shown). In addition, the wild-type folded form of the subunit was restored in the higher Mg^{2+} concentration. For both single mutations, subunit unfolding was reversible, and the folded form was stabilized by Mg^{2+}.

Effects of rRNA Mutations on Translation *in Vivo*. The ability of the mutant ribosomes to participate in translation was monitored by determining the level of mutant rRNA in polyribosomes. The ribosomes from cell lysates were separated on sucrose density gradients and the amount of mutant rRNA in each ribosomal pool was determined by primer

Table 3. Relative levels of mutant rRNA found in various cellular fractions

	rRNA fraction						
			1.5 mM Mg^{2+}*		Lysate†		
Plasmid	Total cellular RNA	Total ribosomes	Unfolded 30S	Folded 30S	30S	70S	Poly-ribosomes
pKK571A	60	56	58	22	80	44	68
pKK865U	60	62	53	38	74	76	67
pKK571A-865U	61	66	74	61	61	68	67

All levels are expressed as the percentage of mutant rRNA in the given sample. Each value represents the mean of at least four measurements. In all cases, standard deviations are <10% of the value reported.

*Samples derived from sucrose density gradients shown in Fig. 3.

†Samples derived from sucrose density gradients shown in Fig. 4.

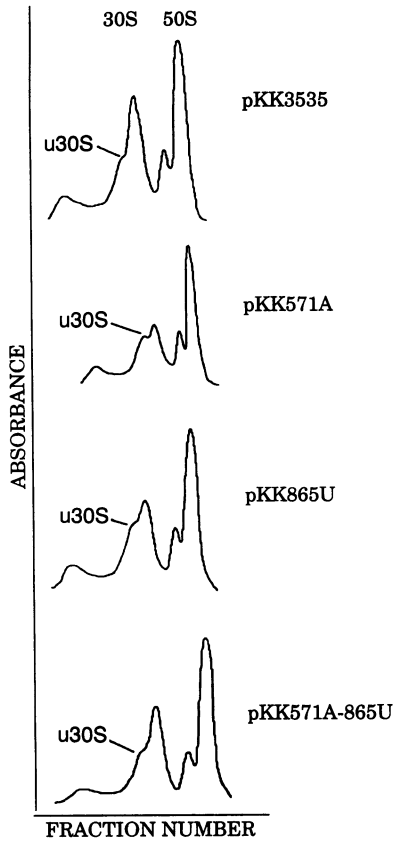

FIG. 3. Sucrose density gradient profiles of ribosomes following dialysis against a low-Mg^{2+} buffer. Samples of isolated ribosomes were dialyzed for 24 hr against a buffer containing 25 mM Tris·HCl (pH 7.6), 1.5 mM $MgCl_2$, and 150 mM KCl. An aliquot containing 2.5 mg of each dialyzed sample was layered onto a 5–30% sucrose density gradient in the same buffer and centrifuged for 20 hr at 24,000 rpm at 4°C in a Beckman SW 28 rotor. Absorbancy of the gradient was monitored at 260 nm. Fractions containing unfolded 30S subunits (u30S) and folded 30S subunits were pooled separately for primer extension analysis.

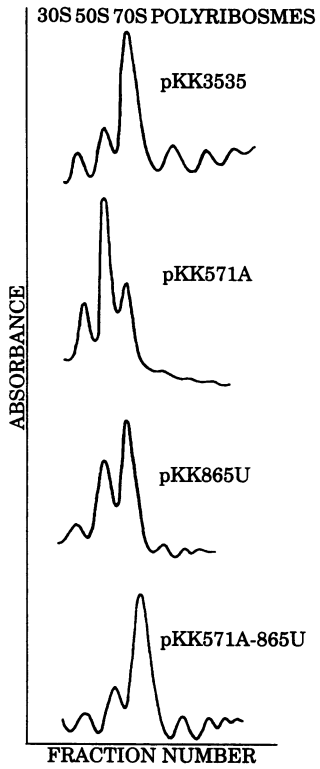

FIG. 4. Sucrose density gradient profiles of cell lysates. Cells were harvested from a 50-ml culture growing at 37°C in LB broth with 200 μg of ampicillin per ml when the OD_{600} reached 0.6. Lysates were prepared as described (20). Half of the lysate was layered onto a 38-ml 5–30% sucrose gradient in 25 mM Tris·HCl, pH 7.6/10 mM $MgCl_2$/60 mM KCl. The gradients were centrifuged at 24,000 rpm for 8 hr at 4°C in a Beckman SW 28 rotor. Fractions corresponding to 30S subunits, 70S ribosomes, or polyribosomes were pooled separately for primer extension analysis.

extension analysis. The A571 mutation led to a significant increase in the amount of free subunits in the polyribosome gradients when compared with wild type (Fig. 4). At the same time, the amount of 70S ribosomes and polyribosomes decreased substantially. The vast majority of rRNA in the large peak of free 30S subunits was mutant rRNA (Table 3). The 70S ribosomes contained very little mutant rRNA and the small quantity of polyribosomes showed a normal level of mutant rRNA. These results indicated that subunits containing the A571 mutation were unstable in 70S ribosomes, and overall the mutant subunits were underrepresented in the translating pool. This interpretation was supported by experiments where the total amount of mutant rRNA in the cell was reduced. When the copy number of pKK571A was lowered so that the total fraction of mutant rRNA in the cell was reduced to 20%, no mutant 30S subunits were detected in either 70S ribosomes or polyribosomes (data not shown). Apparently, the appearance of A571 30S subunits in the translating pool occurred only when a significant amount of the cellular rRNA was mutant.

The gradient profile of the pKK865U lysate differed somewhat from pKK571A (Fig. 4). There was an increase in the size of the free subunit pools, but the increase was much less dramatic. Furthermore, there was no clear exclusion of mutant rRNA from the 70S or polyribosome pools (Table 3). Rather, the U865 subunits were equally represented in all pools, but the overall proportion of ribosomes in translation was reduced. This was most easily observed by noting the reduction in the amount of polyribosomes in the U865 cell lysates.

Subunits containing the double mutation, A571·U865, entered the translating pool efficiently and generated a normal gradient profile (Fig. 4 and Table 3). In addition, mutant rRNA was found in 70S ribosomes and polyribosomes at a level that matched mutant rRNA expression. As in the other assays, the compensatory mutation restored wild-type behavior to the mutant subunits.

DISCUSSION

The results of this study provide experimental support for a pseudoknot interaction in the central domain of 16S rRNA. The tertiary base pair involving positions 571 and 865 is clearly demonstrated by compensatory mutagenesis. Given the strong phylogenetic support for the pairing between residues 570 and 866 (8) and the present study investigating the universally conserved 571·865 pair, the proposed two-base pseudoknot can now join a growing list of experimentally verified higher-order interactions in rRNA. In 16S rRNA this includes the 5′ pseudoknot involving residues 17–19 and 916–918 (6), the pseudoknot involving residues 506–508 and 525–527 (7), and several base pairs involving the 1400- and 1500-position regions (24). In the large subunit, tertiary interactions involving positions 1082 and 1086 in *E. coli* 23S rRNA and positions 1343–1344 and 1403–1404 (*E. coli* numbering) in yeast 26S rRNA have also been supported experimentally (13, 25).

The growth characteristics of cells containing the mutations indicate that the complementarity between 571 and 865 is critically important to the function of the ribosome. At 37°C, the lack of 571·865 complementarity leads to cell death when spectinomycin is present. By restoring the 571·865 complementarity, these cells are rescued to wild-type growth rates. When cell growth is observed at higher and lower temperatures, the effects of the mutations are somewhat more complex. Raising the growth temperature to 42°C might be expected to decrease the stability of the pseudoknot and amplify the slow growth phenotype of the single mutations. Although this occurred for the A571 mutation, cells containing the U865 mutation actually grew somewhat better at 42°C than at 37°C. When the growth temperature was lowered to 30°C, the effects are even more intriguing. While low temperatures would tend to stabilize the pseudoknot structure, both single mutations were extremely deleterious at 30°C. Furthermore, the compensatory double mutation did not rescue growth to the wild-type level. Obviously, base pairing is important for the function of these nucleotides, but additional factors must require more than simple base pairing.

It is not surprising that the single-base mutations at 571 and 865 lead to somewhat different phenotypes given the extremely complex interactions that have been proposed for the rRNA regions surrounding residues 571 and 865. Position 865 is found in a four-nucleotide hairpin loop or tetraloop (26). The tetraloop motif is characterized by extensive hydrogen-bond and stacking interactions among the nucleotides in the loop (27, 28). While the sequence of the 863–866 tetraloop in most Eubacteria (UAAC) does not match the most common of the tetraloop motifs, the primary alternative sequence (GAAA) does fit the consensus (29). In addition, comparative analysis of rRNA sequences in this four-base loop shows covariations typical of tetraloops. While it is apparent that the interactions between nucleotides within tetraloops confer structural stability to RNA hairpins, the detailed role of these motifs in rRNA remains unknown. Perhaps the A-to-U change at 865 disrupts the tetraloop interactions, thereby affecting the folding of the rRNA within the subunit.

The proposed structure of the rRNA surrounding position 571 is even more complex. Comparative sequence analysis supports a lone-pair interaction between G575 and C880 (30). There are also indications that the 910 region may fold into the proximity of 571 through interactions between C564 and G886, G885 and C912, and G887 and C910 (30). Together with the pseudoknot, these interactions would bring several regions of 16S rRNA into the same area in the 30S subunit. Many of these regions have already been localized to a functionally important area where the platform joins the body of the subunit, an area referred to as the cleft. If the central domain pseudoknot forms in the cleft region, it could control the folding of the subunit by changing the relative distance between the platform and the body.

It seems possible that all of the central domain pairings, including the pseudoknot, are not stably formed at all times. Rather, sets of interactions may define alternate conformational states of the subunit. One of these alternate conformations may involve the central domain pseudoknot. The nature of the structural perturbations caused by the 571 and 865 mutations is consistent with a conformational switch. Both single mutations caused a structural unfolding of the 30S subunit at low Mg^{2+} concentrations, but the subunit refolded into a normal structure in the presence of higher concentrations of Mg^{2+}. Thus, the mutations did not preclude proper subunit folding, but rather they destabilized one of the potential folding states. During translation the two states may alternate, stabilized in the more folded state by the pseudoknot.

The functional effects of destabilizing the central domain pseudoknot appear to be dependent on the position of the mutation. When position 571 is mutated, the altered 30S subunits are preferentially excluded from the translating pool. This suggests that the 571 mutation affects the initiation of protein synthesis. Subunits containing a mutation at position 865, on the other hand, are not excluded from translation. These subunits must impair translation at some stage of elongation. Again, there is reason to suspect factors other than simple base pairing are involved in the functional activities of positions 571 and 865.

We thank Matthew Firpo, Michael O'Connor, and Albert Dahlberg for providing strains and engaging in valuable discussions during this work. We are also grateful to Sara Smith-Shull and Patricia Mancuso for technical assistance. This work was supported by National Institutes of Health Grant GM47622.

1. Noller, H. F. (1991) *Annu. Rev. Biochem.* **60,** 191–227.
2. Expert-Benzancon, A. & Wollenzien, P. (1985) *J. Mol. Biol.* **184,** 53–66.
3. Stern, S., Weiser, B. & Noller, H. F. (1988) *J. Mol. Biol.* **204,** 447–481.
4. Schuler, D. & Brimacombe, R. (1988) *EMBO J.* **7,** 1509–1513.
5. Hubbard, J. M. & Hearst, J. E. (1991) *J. Mol. Biol.* **221,** 889–907.
6. Brink, M. F., Verbeet, M. P. & deBoer, H. A. (1993) *EMBO J.* **12,** 3987–3996.
7. Powers, T. & Noller, H. F. (1991) *EMBO J.* **10,** 2203–2214.
8. Gutell, R., Noller, H. F. & Woese, C. R. (1986) *EMBO J.* **5,** 1111–1113.
9. Woese, C. R. & Gutell, R. R. (1989) *Proc. Natl. Acad. Sci. USA* **86,** 3119–3122.
10. Gutell, R. & Woese, C. R. (1990) *Proc. Natl. Acad. Sci. USA* **87,** 663–667.
11. Pleij, C. W. A. (1990) *Trends Biochem. Sci.* **15,** 143–147.
12. Gutell, R. R., Larsen, N. & Woese, C. R. (1993) *Microbiol. Rev.* **58,** 10–26.
13. Kooi, E. A., Rutgers, C. A., Mulder, A., Riet, J. V., Venema, J. & Raue, H. A. (1993) *Proc. Natl. Acad. Sci. USA* **90,** 213–216.
14. Kunkel, T. A. (1985) *Proc. Natl. Acad. Sci. USA* **82,** 488–492.
15. Sanger, F., Nicklen, S. & Coulson, A. R. (1977) *Proc. Natl. Acad. Sci. USA* **74,** 5463–5467.
16. Brosius, J., Ullrich, A., Raker, M. A., Gray, A., Dull, T. J., Gutell, R. R. & Noller, H. F. (1981) *Plasmid* **6,** 112–118.
17. Sigmund, C. D., Ettayebi, M. & Morgan, E. (1984) *Nucleic Acids Res.* **12,** 4653–4663.
18. Makosky, P. & Dahlberg, A. E. (1987) *Biochimie* **69,** 885–890.
19. Tapprich, W. E. & Dahlberg, A. E. (1990) *EMBO J.* **9,** 2649–2655.
20. Godson, N. G. & Sinsheimer, R. L. (1967) *Biochim. Biophys. Acta* **149,** 489–495.
21. Sigmund, C. D., Ettayebi, M., Borden, A. & Morgan, E. (1988) *Methods Enzymol.* **164,** 673–690.
22. Jacob, W., Santer, M. & Dahlberg, A. E. (1987) *Proc. Natl. Acad. Sci. USA* **84,** 4757–4761.
23. Thompson, J., Cundliffe, E. & Dahlberg, A. E. (1988) *J. Mol. Biol.* **203,** 457–465.
24. Cunningham, P. R., Nurse, K., Weitzman, C. J. & Ofengand, J. (1993) *Biochemistry* **32,** 7172–7180.
25. Ryan, P. C. & Draper, D. E. (1991) *Proc. Natl. Acad. Sci. USA* **88,** 6308–6312.
26. Woese, C. R., Winkler, S. & Gutell, R. R. (1990) *Proc. Natl. Acad. Sci. USA* **87,** 8467–8471.
27. Cheong, C., Varani, G. & Tinoco, I. (1990) *Nature (London)* **346,** 680–682.
28. Heus, H. A. & Pardi, A. (1991) *Science* **253,** 191–194.
29. Gutell, R. R. (1993) in *The Translational Apparatus*, eds. Nierhaus, K. H., Subramanian, A. R., Erdmann, V. A., Franceschi, F. & Wittmann-Liebold, B. (Plenum, New York), pp. 477–488.
30. Gutell, R. R. (1994) in *Ribosomal RNA: Structure Evolution, Gene Expression and Function in Protein Synthesis*, eds. Zimmermann, R. A. & Dahlberg, A. E. (CRC, Boca Raton, FL), in press.